



Title	Microstructure in Weld Heat Affected Zone of Al-Mg-Si Alloy(MATERIALS METALLURGY AND WELDABILITY)
Author(s)	Enjo, Toshio; Kuroda, Toshio
Citation	Transactions of JWRI. 1982, 11(1), p. 61-66
Version Type	VoR
URL	<a href="https://doi.org/10.18910/6286">https://doi.org/10.18910/6286</a>
rights	
Note	

*The University of Osaka Institutional Knowledge Archive : OUKA*

<https://ir.library.osaka-u.ac.jp/>

The University of Osaka

# Microstructure in Weld Heat Affected Zone of Al-Mg-Si Alloy†

Toshio ENJO\* and Toshio KURODA\*\*

## Abstract

*An investigation has been made into the microstructure of weld heat affected zone (HAZ) in commercial Al-Mg-Si system 6063-T5 alloy.*

*The precipitation amounts of G.P. zones,  $\beta'$  precipitates,  $\beta$  phase and relatively insoluble compounds respectively in the HAZ can be evaluated quantitatively by means of electrical resistivity measurement of an isochronal annealing technique.*

*The partial or all dissolution of G.P. zones and  $\beta'$  precipitates occurs in a narrow band of the HAZ where the temperature has reached above 240°C during welding.*

*The softening zone remains in these parts of HAZ in spite of natural aging after welding. The softening zone can be considerably improved by means of artificial aging treatment at 180°C for 8 hours after welding.*

**KEY WORDS:** (Al-Mg-Si Alloy) (Heat Affected Zone) (Electrical Resistivity) (Metallography)

## 1. Introduction

Al-Mg-Si system 6063 alloy has characterized by ease of extrusion and has widely used as the structural materials for welds. This alloy is the precipitation hardening alloy, and the high strength is maintained by artificial aging after solution treatment.

It is found that generally this alloy is difficult to weld. The difficulty arises from the weld thermal cycle destroying the precipitation hardened structure in the weld zone and in the parent metal adjacent to the fusion zone, and then the softening zones occur in the weld heat affected zone (HAZ), which the hardness is lower than that of another area.

The basal aging process of this alloy is explained as follows.<sup>1)</sup>

Cluster (G.P. (I) zone)→Acicular G.P. zones (G.P. (II) zone)→Rod shape intermediate phase ( $\beta'$  precipitates)→Plate shape equilibrium phase ( $\beta$  phase)  $\beta$  phase is indicated as  $Mg_2Si$ ,  $\beta'$  precipitates and G.P. zones contained in this alloy generally contribute to hardness.

In this paper, as the alloy is welded, the precipitation behavior in the HAZ has been investigated by means of electrical resistivity measurement and transmission electron microscopy. And then the amount of G.P. zones and  $\beta'$  precipitates in the HAZ has been evaluated quantitatively by electrical resistivity, and the mechanism of softening zone has been discussed.

## 2. Experimental Procedure

The material used in this investigation is commercially Al-Mg-Si system 6063-T5 alloy with 6 mm thickness. The chemical compositions are shown in **Table 1**.

The plate used has been cut into 130 mm wide and 200 mm long. The bead on plate welds were made in the middle of the plate using DCSP-TIG process in a argon gas. The welding condition is shown in **Table 2**. Now, the Copper plate 250 mm wide, 500 mm long and 10 mm thick was used as the backing plate in order to suppress the whole test plate to be heated up.

**Table 1** Chemical compositions of material used (wt%)

Material	Cu	Si	Fe	Mn	Mg	Zn	Cr	Ti	Zr	Al
6063-T5	tr.	0.42	0.19	0.02	0.56	0.01	tr.	0.02	-	Bal.

**Table 2** Welding condition

Current (A)	Voltage (V)	Welding Speed (cm/min)	Heat Input (J/cm)
180	18	18.8	10300

The precipitation phenomena of the alloy was carried out using electrical resistivity measurement and transmission electron microscopy. Thin foils for transmission electron microscopy were prepared using a jet polishing technique. The thin plates for electrical resistivity measurement were cut into strips 35 mm long, 2 mm wide and 0.5 mm thick using electric discharge machine.

The electrical resistivity measurements were made in liquid nitrogen at -196°C by conventional potentiometric method shown in **Fig. 1**. The heat treatment of the plate of welds and base metal was made using

† Received on March 31, 1982

\* Professor

\*\* Research Instructor

Transactions of JWRI is published by Welding Research Institute of Osaka University, Ibaraki, Osaka, Japan

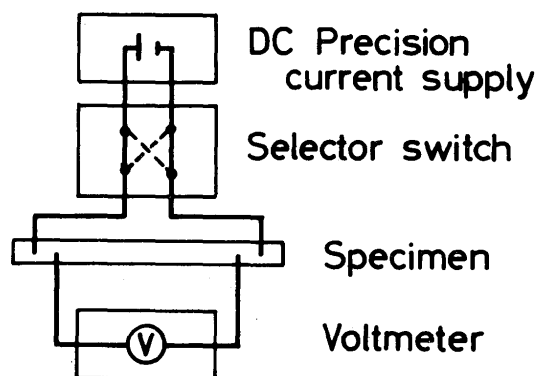


Fig. 1 Schematic diagram of electrical resistivity measurement by conventional potentiometric method.

the silicone oil bath and the salt bath.<sup>2)</sup> The temperatures used were controlled to within  $\pm 2^\circ\text{C}$ .

### 3. Results and Discussion

#### 3.1 The method of quantitative evaluation of microstructure in the HAZ

As the 6063-T5 alloy was welded, G.P. zones and  $\beta'$  precipitates contained in the alloy generally precipitate or solutionize in the HAZ. Figure 2 shows the change in resistivity and hardness as the 6063-T5 alloy was heated for 10 minutes at each temperature up to  $560^\circ\text{C}$  respectively, that is as the isochronal annealing was made. The hardness is constant in the temperature range from  $0^\circ\text{C}$  to  $240^\circ\text{C}$ . Above the temperature, the hardness decreases with increasing temperature up to  $360^\circ\text{C}$ . And then, the hardness is about constant above  $360^\circ\text{C}$ .

The resistivity is constant in the temperature range from  $0^\circ\text{C}$  to  $160^\circ\text{C}$ , but decreases with increasing

temperature at above  $160^\circ\text{C}$  up to  $300^\circ\text{C}$ , and the resistivity increases with increasing the temperature in the range from  $300^\circ\text{C}$  to  $380^\circ\text{C}$ , and decreases at the temperature range of  $380^\circ\text{C}$  to  $420^\circ\text{C}$ .

Above  $420^\circ\text{C}$ , the resistivity increases with increasing temperature up to  $500^\circ\text{C}$ . And then at  $500^\circ\text{C}$ , the resistivity shows constant value.

Such a resistivity change depends on the concentration change of Mg and Si in solution in the matrix due to the precipitates such as  $\text{Mg}_2\text{Si}$ . This resistivity change is corresponded to the results of specific heat measurement.<sup>4)</sup>

In the resistivity of Fig. 2, the resistivity change due to G.P. zones is indicated by  $\Delta\rho_1$ , the change due to  $\beta'$  precipitates is indicated by  $\Delta\rho_2$ , the change due to  $\beta$  phase is  $\Delta\rho_3$  and the change due to relatively insoluble compounds is indicated by  $\Delta\rho_4$ .

Figure 3 shows the transmission electron micrographs of various typical precipitates in the 6063 alloy. Acicular or spherical G.P. zones precipitate finely, and a little relatively insoluble compounds and  $\beta'$  precipitates occurs in the as-received (T5) material as shown in Fig. 3-(a). When the sample was inclined about 10 degree to the electron beam direction, the strain contrast due to G.P. zones formation is observed, as shown in Fig. 3-(b). And the diffraction pattern was carried out, as the results, the patterns were indicated the spot with streaks.

Next, the 6063 alloy was solution-treated, water quenched, and then aged at  $280^\circ\text{C}$  for 4.5 hours. The microstructure obtained by the heat treatment is indicated as shown in Fig. 3-(c). Rod shape  $\beta'$  precipitates occur and the relatively insoluble compounds are partially observed. Figure 3-(d) shows the transmission electron micrograph as the alloy was aged at  $400^\circ\text{C}$  for 2 hours after solution treatment.  $\beta$  phase of plate shape precipitates.

Such a result is corresponded to the result of Thomas.<sup>3)</sup> G.P. zones,  $\beta'$  precipitates,  $\beta$  phase and relatively insoluble compounds respectively can be observed by transmission electron microscopy. When the alloy is aged at room temperature after solution treatment, the cluster due to Mg and Si generates, the generation of cluster can be measured by means of electrical resistivity measurement only.

The relation between resistivity changes due to the precipitates and increment of hardness is shown in Fig. 4.  $\beta$  phase hardly contributes to hardness. The cluster contributes to hardness up to Hv 7. But G.P. zones aged at  $180^\circ\text{C}$  and  $\beta'$  precipitates aged at  $280^\circ\text{C}$  respectively contribute to hardness considerably. Consequently,  $\beta'$  precipitates and G.P. zones strongly

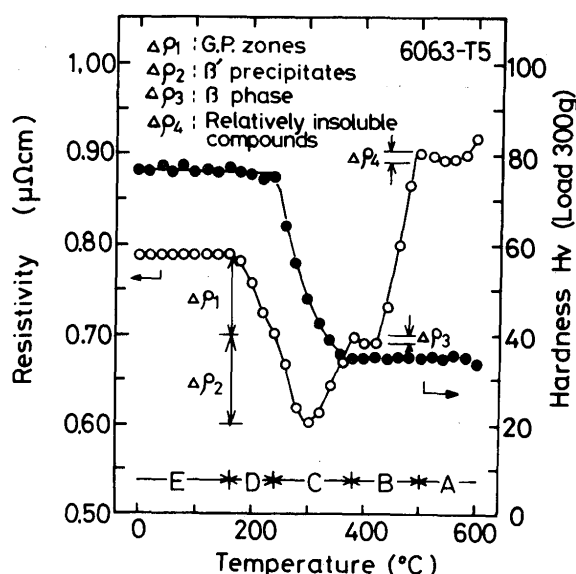


Fig. 2 Isochronal annealing curves of electrical resistivity and hardness for 6063-T5 alloy.

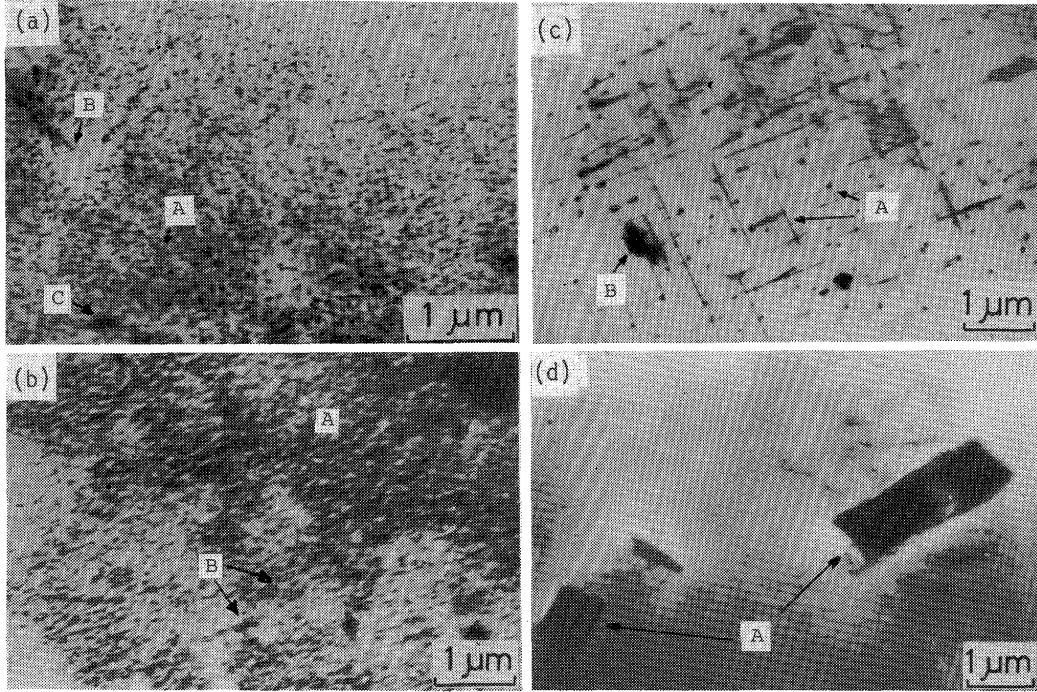


Fig. 3 Transmission electron micrographs of various precipitates in 6063 alloy.

- (a), (b) As received (T5) A: G.P. Zones B:  $\beta'$  precipitates C: Relatively Insoluble Compounds  
 (c) Aged at 280°C for 4.5 hrs after solution treatment at 560°C for 2 hrs. A:  $\beta'$  precipitates B: relatively insoluble compounds  
 (d) Aged at 400°C for 2 hrs. A:  $\beta$  phase.

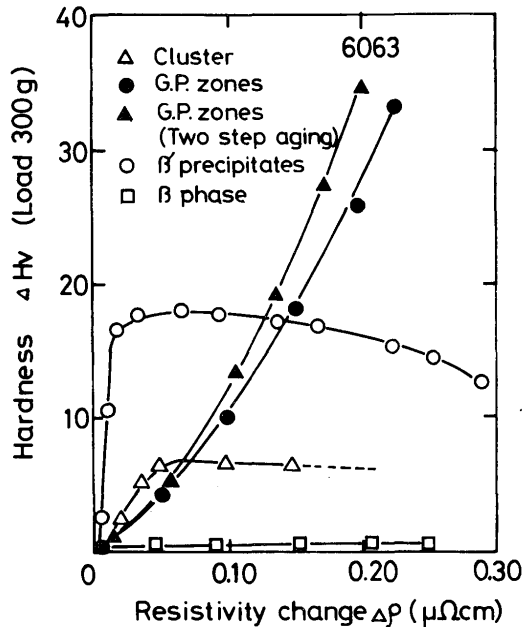


Fig. 4 Relation between resistivity change due to precipitation and increment of hardness for various precipitates in 6063 alloy.

contributes to the hardness in Al-Mg-Si system 6063 alloy.

Figure 5 shows the relation between  $\Delta\rho_1'$  by 180°C isothermal aging and  $\Delta\rho_1$  in isochronal annealing curve. The  $\Delta\rho_1'$  is related to the formation of G.P. zones. The  $\Delta\rho_1$  decreases with increasing the  $\Delta\rho_1'$ . That is, as the sample contained G.P. zones more is isochronal-

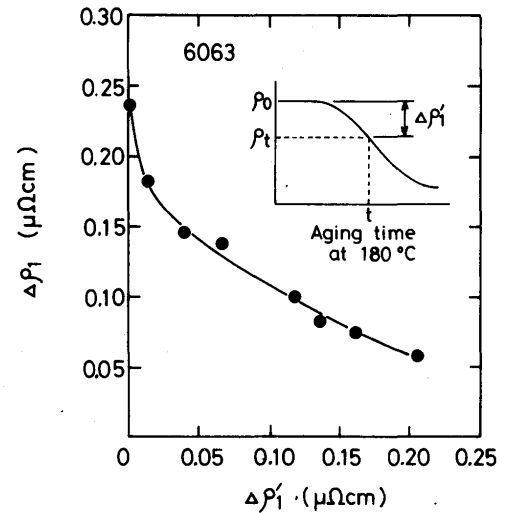


Fig. 5 Relation between  $\Delta\rho_1'$  by 180°C isothermal aging and  $\Delta\rho_1$  in isochronal annealing curve for 6063 alloy.

annealed, the  $\Delta\rho_1$  is low, it means that the formation of G.P. zones during isochronal annealing is a little.

Figure 6 shows the relation between  $\Delta\rho_2'$  by 280°C isothermal aging and  $\Delta\rho_2$  in isochronal annealing curve for 6063 alloy. The  $\Delta\rho_2'$  is related to the  $\beta'$  precipitation. The  $\Delta\rho_2$  decreases with increasing the  $\Delta\rho_2'$ . That is, the  $\Delta\rho_2$  of the sample that  $\beta'$  precipitates solutionized is high.

Consequently,  $\Delta\rho_1$ ,  $\Delta\rho_2$ ,  $\Delta\rho_3$ , and  $\Delta\rho_4$  depend on the precipitation amount of G.P. zones,  $\beta'$  precipitates,  $\beta$  phase and relatively insoluble compounds respectively

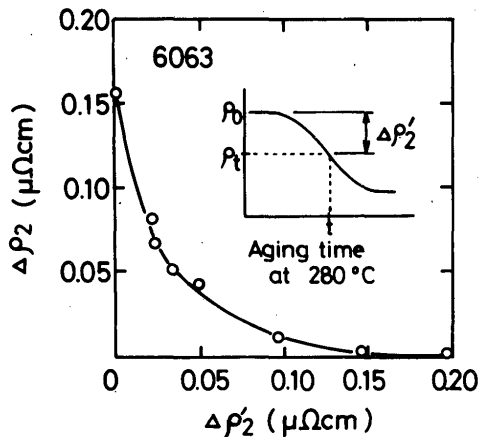


Fig. 6 Relation between  $\Delta\rho_2'$  by 280°C isothermal aging and  $\Delta\rho_2$  in isochronal annealing curve for 6063 alloy.

before isochronal annealing.

But  $\Delta\rho_1$ ,  $\Delta\rho_2$ ,  $\Delta\rho_3$ , and  $\Delta\rho_4$  respectively is the value precipitated during isochronal annealing, and this value is not really indicated the precipitation amount of the various precipitates occurred in the HAZ during welding, before isochronal annealing.

In the HAZ, the precipitation temperature range of the G.P. zones and  $\beta'$  precipitates are generally wide.<sup>4)</sup> In a short time, G.P. zones form at 160°C to 240°C, and  $\beta'$  precipitates occur at about 240°C to 380°C as shown in Fig. 2. G.P. zones form mostly at 180°C,  $\beta'$  precipitates occur mostly at 280°C. Then, the precipitation amounts of G.P. zones ( $\Delta\rho_1'$ ) and  $\beta'$  precipitates ( $\Delta\rho_2'$ ) can be evaluated by substituting  $\Delta\rho_1$  and  $\Delta\rho_2$  to Fig. 5 and Fig. 6.

Concerning  $\beta$  phase ( $\Delta\rho_3'$ ) and relatively insoluble compounds ( $\Delta\rho_4'$ ), their values are evaluated, based on the T5 material.

### 3.2 Quantitative evaluation of microstructure in weld heat affected zone

Figure 7 shows the distribution of hardness when

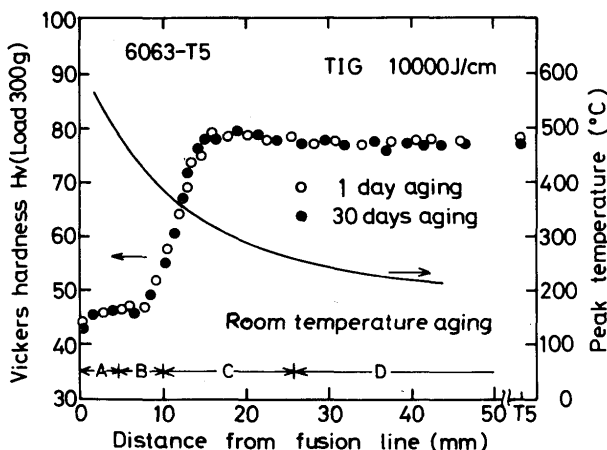


Fig. 7 Distribution of hardness and peak temperature on TIG welds for 6063-T5 alloy.

6063-T5 plate was welded using TIG method. The hardness decreases to Hv 45 in the range from the fusion line to 8 mm in the HAZ. The hardness decreases with decreasing the distance from fusion line in the range of 8 mm to 14 mm from the fusion line in the HAZ. The hardness of the region 14–30 mm from the fusion line is fairly higher than that of as-received (T5) material, and the hardness so far the region 30 mm from the fusion line in the HAZ is same as that of as-received (T5) material.

Figure 8 shows the distribution of electrical resistivity change in TIG welds of 6063-T5 alloy. The  $\Delta\rho$  of the HAZ is larger than that of as-received. And it means that the precipitation amount in the HAZ was more than that of as-received (T5) material.

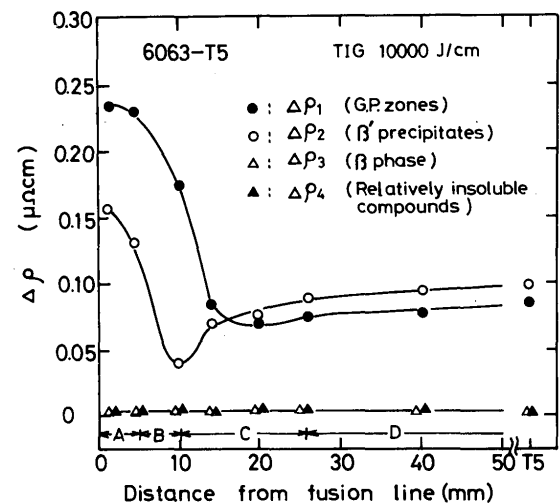


Fig. 8 Distribution of electrical resistivity change in TIG welds of 6063-T5 alloy.

Concerning the  $\Delta\rho_1$ , the  $\Delta\rho_1$  of as-received (T5) material is 0.088  $\mu\Omega\text{cm}$ , that of region 14–26 mm from fusion line in the HAZ is about 0.075  $\mu\Omega\text{cm}$ . It means that G.P. zones form more than that of as-received (T5) material. The  $\Delta\rho_1$  in the range of the region 14 mm from fusion line in the HAZ is larger than that of as-received (T5) material, it means that G.P. zones are considerably solutionized.

Concerning  $\beta'$  precipitates, the  $\Delta\rho_2$  of the region 10–40 mm from fusion line in the HAZ is lower adjacent to the fusion line, it means that  $\beta'$  precipitates occurs more than that of as-received (T5) material. The  $\Delta\rho_3$  and the  $\Delta\rho_4$  hardly change as well as that of as-received (T5) material. And then, in order to evaluate the microstructure change in the HAZ, the  $\Delta\rho_1$  and the  $\Delta\rho_2$  was put into the  $\Delta\rho_1'$  and the  $\Delta\rho_2'$  in the curves of Fig. 5 and Fig. 6.

Figure 9 shows the distribution of G.P. zones ( $\Delta\rho_1'$ ),  $\beta'$  precipitates ( $\Delta\rho_2'$ ),  $\beta$  phase ( $\Delta\rho_3'$ ) and relatively insoluble compounds ( $\Delta\rho_4'$ ) in the HAZ of TIG welds

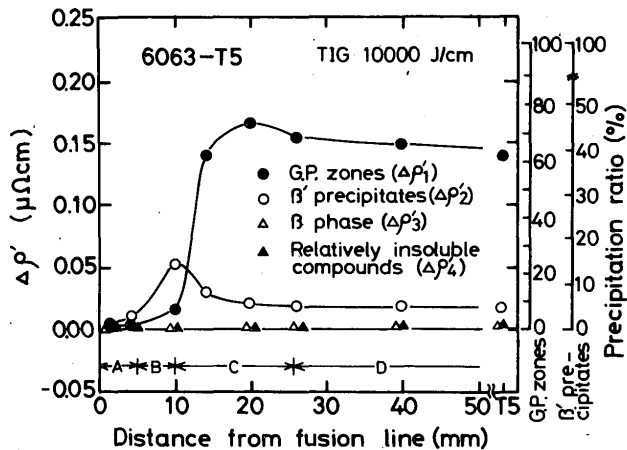


Fig. 9 Distribution of G.P. Zones ( $\Delta\rho_1'$ ),  $\beta'$  precipitates ( $\Delta\rho_2'$ ),  $\beta$  phase ( $\Delta\rho_3'$ ) and relatively insoluble compounds ( $\Delta\rho_4'$ ) in the HAZ of TIG welds of 6063-T5 alloy.

of 6063-T5 alloy. The relatively insoluble compounds ( $\Delta\rho_4'$ ) and  $\beta$  phase ( $\Delta\rho_3'$ ) are same precipitation amount as well as as-received (T5) material.

Concerning G.P. zones, the  $\Delta\rho_1'$  is larger than that of as-received (T5) material at the region 15–40 mm from fusion line in the HAZ. Concerning  $\beta'$  precipitates, the  $\Delta\rho_2'$  of as-received (T5) material is  $0.018 \mu\Omega\text{cm}$ , and that of 10 mm from the fusion line in the HAZ is  $0.05 \mu\Omega\text{cm}$ . Consequently in this region, it means that  $\beta'$  precipitates occurred more than that of as-received (T5) material.

The precipitation amount of G.P. zones is 62% ( $0.14 \mu\Omega\text{cm}$ ) of whole precipitation amount ( $0.23 \mu\Omega\text{cm}$ ), that of  $\beta'$  precipitates is 5% ( $0.018 \mu\Omega\text{cm}$ ) of whole precipitation amount ( $0.36 \mu\Omega\text{cm}$ ) for as-received (T5) material. At the region 10 mm from fusion line in the HAZ,  $\beta'$  precipitates is 14% ( $0.05 \mu\Omega\text{cm}$ ) and G.P. zones is 8% ( $0.016 \mu\Omega\text{cm}$ ). It means that G.P. zones is little but  $\beta'$  precipitates occurs considerably in this region. At the region 14 mm from the fusion line in the HAZ, G.P. zones is 62% ( $0.14 \mu\Omega\text{cm}$ ) of whole G.P. zones precipitation ( $0.23 \mu\Omega\text{cm}$ ),  $\beta'$  precipitates is 13% ( $0.03 \mu\Omega\text{cm}$ ) of whole  $\beta'$  precipitation, it means that the amount of G.P. zones is less than that of as-received (T5) material in the region.

Figure 10 shows the transmission electron micrographs in the HAZ of TIG welds for 6063-T5 alloy. G.P. zones is hardly observed and  $\beta'$  precipitates is more than that of as-received (T5) alloy in the region of 10 mm from fusion line in the HAZ, and  $\beta$  phase is observed a little. This results of the observation is corresponded to Fig. 8.

Acicular G.P. zones and rod shape  $\beta'$  precipitates are observed. G.P. zones is less and  $\beta'$  precipitates is more than that of as-received (T5) material. This

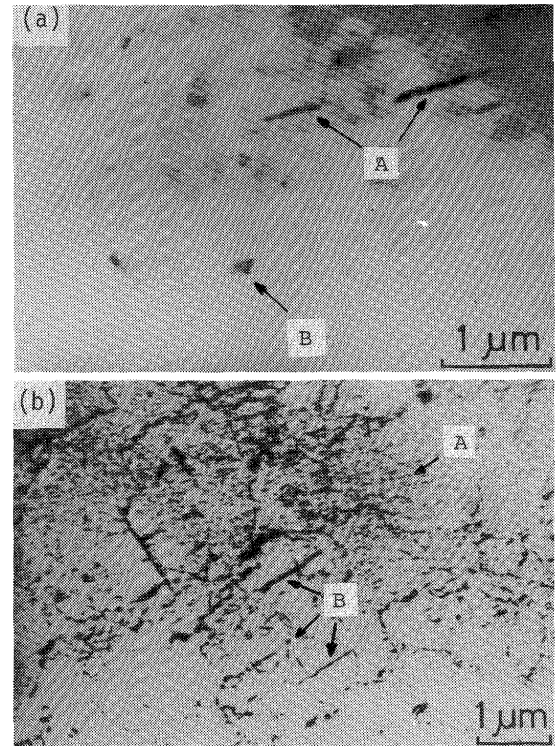


Fig. 10 Transmission electron micrographs in the HAZ of TIG welds for 6063-T5 alloy.

(a) HAZ of 10 mm from fusion line. (A:  $\beta'$  precipitates, B:  $\beta$  phase) (b) HAZ of 14 mm from fusion line. (A: G.P. Zones, B:  $\beta'$  precipitates)

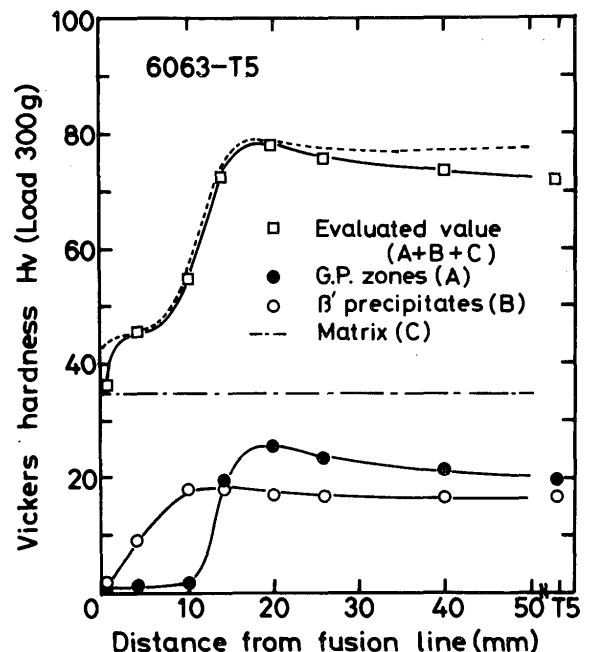


Fig. 11 Distribution of hardness due to G.P. Zones,  $\beta'$  precipitates and the matrix in TIG welds of 6063-T5 alloy.

results are corresponded to that of Fig. 8 at the region of 14 mm from the fusion line in the HAZ.

Figure 11 shows the distribution of hardness due to G.P. zones,  $\beta'$  precipitates and the matrix in TIG

welds of 6063-T5 alloy. This is obtained by substituting G.P. zones ( $\Delta\rho_1'$ ) and  $\beta'$  precipitates ( $\Delta\rho_2'$ ) in Fig. 9 to G.P. zones ( $\Delta\rho$ ) (Two step aging) and  $\beta'$  precipitates ( $\Delta\rho$ ) in Fig. 4. The hardness due to G.P. zones decreases with increasing the distance from the fusion line compared to  $\beta'$  precipitates, because that solvus temperature of G.P. zones is lower than that of  $\beta'$  precipitates.  $\beta'$  precipitates contribute to hardness significantly.

Consequently, this alloy (T5) is the mixture structure of G.P. zones and  $\beta'$  precipitates, the hardness is considered to appear by their sum of the precipitates. The hardness of matrix after solution treatment was Hv 35. The hardness of the matrix, G.P. zones and  $\beta'$  precipitates are summarized up and the results are indicated by symbol  $\square$ . This results are corresponded to the results of Fig. 7.

### 3.3 Improvement of softening zone in the HAZ by post weld heating

Figure 12 shows the hardness recovery due to artificial aging at 180°C for 8 hours after welding for 6063-T5 alloy.

The hardness is same as that of as-received (T5) material at the region 14–50 mm from the fusion line in the HAZ. But the hardness doesn't restore only up to Hv 10 at the region 10 mm from the fusion line in the HAZ. This softening zone is related to the  $\beta'$  precipitation occurred during welding.

Consequently,  $\beta'$  precipitates are considered to suppress the precipitation of G.P. zones due to artificial aging after welding. But, the hardness decreasing area of Hv 45 is improved up to Hv 70 by artificial aging after welding.

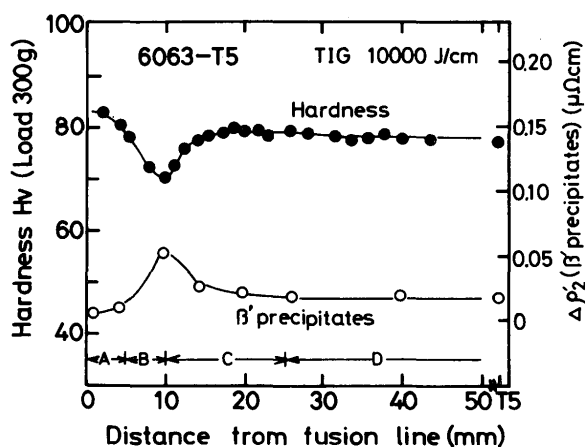


Fig. 12 Hardness recovery due to artificial aging at 180°C for 8 hrs after welding for 6063-T5 alloy.

## 4. Conclusion

An investigation has been made into the micro-

structure in the weld heat affected zone of 6063-T5 alloy by means of electrical resistivity measurement and transmission electron microscopy. The results obtained in this investigation are summarized as follows.

- 1) The microstructure change in the weld heat affected zone can be evaluated quantitatively using isochronal annealing technique of electrical resistivity.
- 2) The precipitation behavior of G.P. zones,  $\beta'$  precipitates,  $\beta$  phase and relatively insoluble compounds by electrical resistivity respectively is corresponded to the results of transmission electron microscopy.
- 3) By means of electrical resistivity measurement, the alloy has mixture structure of G.P. zones and  $\beta'$  precipitates, and G.P. zones and  $\beta'$  precipitates is considerably contributed to hardness. The alloy is welded, the softening zone occurs in the region adjacent to the fusion line in the HAZ, because of the solution of G.P. zones and  $\beta'$  precipitates.
- 4) The softening zone is considerably improved by artificial aging at 180°C for 8 hours after welding. But the hardness restoration is suppressed in the region of the precipitation of  $\beta'$  precipitates. The suppression of the formation of G.P. zones by the artificial aging occurs due to the precipitation of  $\beta'$  precipitates during welding.

## Acknowledgement

The authors wish to thank Mr. M. Mishima for his variable contribution in this work. The support of the Light Metal Educational Foundation is greatly acknowledged.

## References

- 1) C. Panseri and T. Federighi; A Resistometric Study of Precipitation in an Aluminum-1.4% Mg<sub>2</sub>Si Alloy, J. Inst. Metals, 54 (1966), 99-107.
- 2) T. Enjo and T. Kuroda; Effect of Relatively Insoluble Compounds on  $\beta$  phase Precipitation of 5083 Aluminum Alloy, Trans. JWRI 7-2 (1978), 25.
- 3) G. Thomas; The aging Characteristics of Aluminum Alloys, J. Inst. Metals, 90 (1961-62), 57-63.
- 4) T. Miyauchi, S. Fujikawa and K. Hirano; Precipitation Process of Al-Mg-Si Alloys by Ageing, J. Japan Inst. Light Metals, 21-9 (1971), 595 (In Japanese).
- 5) S. Khoda; Gokin no Sekisyutsu, 404-419, Maruzen, Tokyo (In Japanese)